

Article

# Shear Stress-Based Analysis of Sediment Incipient Deposition in Rigid Boundary Open Channels

Necati Erdem Unal 

Department of Civil Engineering, Hydraulics Division, Istanbul Technical University, Maslak, 34469 Istanbul, Turkey; neu@itu.edu.tr; Tel.: +90-212-285-3727

Received: 24 September 2018; Accepted: 4 October 2018; Published: 9 October 2018



**Abstract:** Urban drainage and sewer systems, and channels in general, are treated by the deposition of sediment that comes from water collecting systems, such as roads, parking lots, land, cultivation areas, and so forth, which are all under gradual or sudden change. The carrying capacity of urban area channels is reduced heavily by sediment transport that might even totally block the channel. In order to solve the sedimentation problem, it is therefore important that the channel is designed by considering self-cleansing criteria. Incipient deposition is proposed as a conservative method for channel design and is the subject of this study. With this aim, an experimental study carried out in trapezoidal, rectangular, circular, U-shape, and V-bottom channels is presented. Four different sizes of sand were used as sediment in the experiments performed in a tilting flume under nine different longitudinal channel bed slopes. A shear stress approach is considered, with the Shields and Yalin methods used in the analysis. Using the experimental data, functionals are developed for both methods. It is seen that the bed shear stress changes with the shape of the channel cross-section. Incipient deposition in rectangular and V-bottom channels starts under the lowest and the highest shear stress, respectively, due mainly to the shape of the channel cross-section that affects the distribution of shear stress on the channel bed.

**Keywords:** incipient deposition; sediment transport; self-cleansing; sewer systems; shear stress; urban drainage system

## 1. Introduction

The sediment transport issue has always been an important scientific and practical problem [1,2], and kept its importance with the changes in hydrology [3–5] emerging with the change in the sediment load of urban watersheds and alluvial streams. As the outlets of urban watersheds, the sewer and urban drainage systems are heavily affected by any change in their watersheds. Therefore, research on sediment transport is continuously needed for sustainable practice in drainage systems.

Sediment deposition is avoided as it causes numerous unwanted problems in urban drainage and sewer systems. It reduces the hydraulic capacity of the channel by decreasing the flow cross-sectional area or blocking the channel. The performance and efficiency of drainage systems is heavily affected by deposition. Additional funds should be invested to keep the system working. Furthermore, sedimentation creates environmental problems. Such problems in drainage and sewer systems could be prevented or minimized by the use of self-cleansing criteria, with which sediment particles deposited at the channel bed start to move [6], or sediment particles suspended within the flow are transported without being deposited [7–9]. Transportation of sediment particles without deposition is preferred in drainage system design to keep the channel bed clean [10–14]. In this regard, incipient deposition is a concept linked to the channel design, and identified as the sediment transport mode in which sediment particles are clustered visibly in certain areas at the channel bed [15]. In other words, sediment particles are transported as bed load or accumulated at the channel bed, but without making a permanent

deposited bed layer [15–17]. Flow velocity is sufficiently low for incipient deposition of sediment. At the incipient deposition, sediment particles in suspension within flow start moving downward to reach the channel bed.

Incipient deposition has been studied in several fixed bed channels by Loveless [15] who assumed that incipient motion and incipient deposition were similar concepts but with a slight difference [18]. The experimental data of Loveless [15] fit the sediment transport models of May [19] and Ackers [20]. Safari et al. [16] studied the incipient deposition concept using the experimental data of Loveless [15]. As a conclusion, velocity at incipient deposition was found to be higher than velocity at incipient motion for non-cohesive sediments. Incipient deposition is observed when flow velocity decreases gradually to a level that allows sediment particles to deposit. In the opposite case, when flow velocity increases gradually, sediment particles with no motion start moving when flow velocity reaches a level high enough for incipient motion. The former is called the incipient deposition velocity, which is higher than the latter, the incipient motion velocity. This is a hysteretic curve with a higher threshold velocity for incipient deposition and lower threshold velocity for the incipient motion. In this paradigm, there is a shear stress (or velocity) threshold below which erosion does not occur, and a lower threshold above which deposition does not occur; erosion and deposition occur simultaneously between the two thresholds [21]. Therefore, results denied the common assumption that incipient deposition and incipient motion are the same.

In order to explain the exact difference between the incipient deposition and incipient motion, Aksoy and Safari [22] performed a preliminary study on incipient motion and incipient deposition in a trapezoidal cross-section channel, and found that the flow has higher shear stress at incipient deposition than at the incipient motion. For the sake of achieving more conclusive results, a new set of experiments with a wider range of sediment size in different channel cross-sections seemed important. Not only because of its importance, but also for the sake of getting experimental data with a wider range in terms of sediment size, channel cross-section, channel slope, discharge, and so forth, Unal et al. [23] constructed a laboratory experimental setup to study the incipient motion and incipient deposition in trapezoidal, rectangular, circular, U-shape, and V-bottom channels, and performed experiments for the self-cleansing design of fixed bed systems.

In this study, experimental data from an indoor laboratory flume was analyzed to understand the incipient deposition of sediment particles within flow. The shear stress approach was considered for the analysis in which the Shields [24] and Yalin [25] methods were used.

## 2. Mechanism of Particle Motion and Methodology

Sediment particles in flow move under the influence of two types of hydrodynamic forces; the first of which has a positive impact through the drag force and the lift force, while the second discourages motion through the buoyed weight of sediment and the resisting force against motion. The drag force should be equal to the resistance force in the sediment threshold condition.

The shear stress- and velocity-based approaches were commonly used in the analysis of sediment threshold and incipient deposition in this study. The velocity-based approach has been applied on the experimental data existing in the literature [26]. The shear stress approach was used in this study for which Shields [24] and Yalin [25] methods are considered.

### 2.1. Shields Method

The shear stress approach used in the incipient deposition of sediment is based on the shear velocity ( $u_*$ ), defined as

$$u_* = \sqrt{\frac{\tau_{id}}{\rho}} \quad (1)$$

in which  $\tau_{id}$  is the bed shear stress under the incipient deposition condition and  $\rho$  is the specific mass of water. The dimensionless shear stress is calculated by

$$\tau_{id}^* = \frac{\tau_{id}}{\rho g d (s - 1)}. \quad (2)$$

in which  $g$  is the acceleration due to gravity,  $d$  is the median size of sediment particles, and  $s$  is the sediment relative mass density. The dimensionless shear stress ( $\tau_{id}^*$ ) is indicated as

$$\tau_{id}^* = f(Re^*) \quad (3)$$

where  $Re^*$  is the particle Reynolds number ( $Re^*$ ) defined by

$$Re^* = \frac{u_* d}{\nu} \quad (4)$$

in which  $\nu$  is the kinematic viscosity of water.

Experimental data has been used by many researchers [9,15–17,22,23,26] to determine the functional between  $\tau_{id}^*$  and  $Re^*$  for practical problems of incipient motion [27,28]. In this study, the same methodology was adopted for the incipient deposition.

Average flow velocity ( $V_{id}$ ) calculated from the incipient deposition experimental data is used to calculate the incipient deposition shear stress by

$$\tau_{id} = \frac{\lambda \rho V_{id}^2}{8} \quad (5)$$

in which  $\lambda$  is the channel friction factor to be calculated by the Colebrook–White equation [29] as

$$\lambda = \frac{1}{4 \left[ \log \left( \frac{k_b}{14.8R} + \frac{0.22\nu}{R\sqrt{gRS}} \right) \right]^2} \quad (6)$$

in which  $k_b$  is the roughness height of the bed taken to be the same as the median size of sediment particles ( $d$ ),  $R$  is the hydraulic radius of the channel, and  $S$  is the slope of the channel bed.

## 2.2. Yalin Method

Yalin [25] suggested a combination of the dimensionless parameters initially proposed by Shields [24] as

$$\tau_{id}^* = f(D_{gr}) \quad (7)$$

in which  $D_{gr}$  is the dimensionless grain size parameter defined by

$$D_{gr} = \left[ \frac{(s - 1)gd^3}{\nu^2} \right]^{1/3} \quad (8)$$

The shear velocity is eliminated, and only fluid and sediment characteristics are retained in the formulation.

## 3. Experiments

An experimental setup was configured as in Figure 1 [22,23]. An iron-made support structure was constructed. Twelve meter-long transparent acrylic glass (plexiglass) channels were mounted on the support structure. Five different cross-sections were considered for the channels; they were trapezoidal, rectangular, circular, U-shape, and V-bottom. The surface width of the rectangular, U-shape, and V-bottom channels was 300 mm, while the trapezoidal channel had the same width at

the bottom, and outer angles of 60° at the 30 cm-long side walls. The U-shape and V-bottom channels had a cross-fall of 50 mm longitudinally along the centerline of the bottom. The inner diameter of the circular channel was 290 mm.

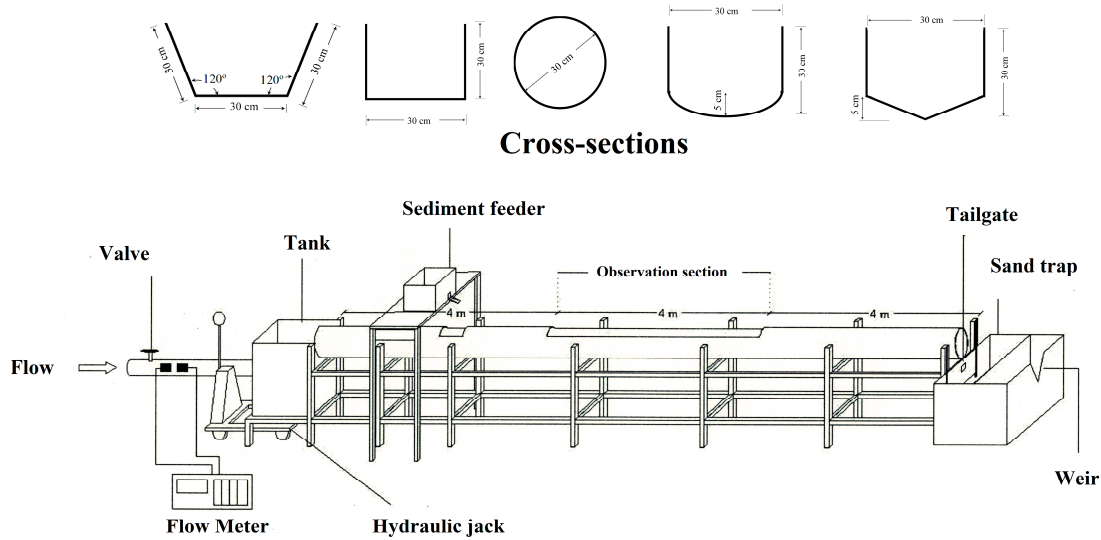


Figure 1. Experimental setup and cross-sections of the channels.

In the experiments, the bed slope was changed between 0.00147 and 0.01106. Four non-cohesive sands were poured into the channel from the sediment feeder placed 3 m upstream of the observation section of the channel. The granulometric curve and the characteristics of the sands are shown in Figure 2 and Table 1, from which it can be seen that they have uniform size distribution. The discharge was measured by an ultrasonic flowmeter (BSUF-TTCL, Bass Instruments, Istanbul, Turkey) with an accuracy better than 1.0% of read. Sediment motion was observed in each experiment in the 4 m-long observation section of the channel, 4 m from the inlet and 4 m from the outlet of the channel (Figure 1). Uniform flow conditions were satisfied in the channel before observations and measurements were done.

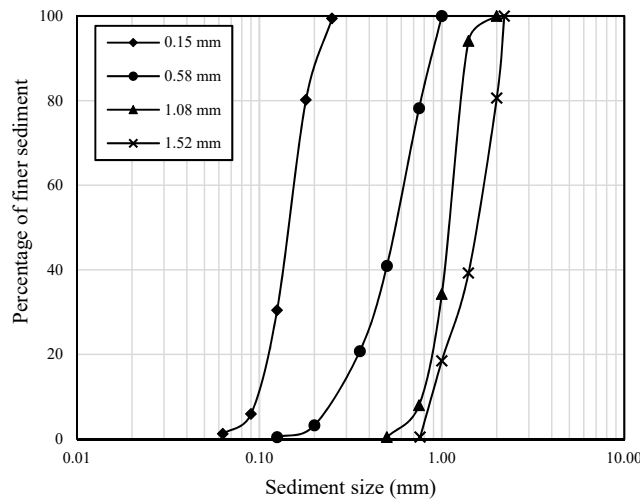


Figure 2. Granulometric curve of sediment.

**Table 1.** Sediment characteristics. *d*: median diameter, *s*: relative mass density,  $\sigma_g$ : geometric standard deviation of sediment particles.

<i>d</i> (mm)	0.15	0.58	1.08	1.52
<i>s</i>	2.60	2.63	2.56	2.60
$\sigma_g$	1.3	1.6	1.3	1.4

Experiments started with a flow velocity high enough to achieve the non-deposition condition. The average velocity was adjusted by increasing or decreasing flow discharge into the channel. In the non-deposition condition, sediment particles are prevented from being deposited; that is, sediment particles within flow are in motion. Flow velocity was gradually decreased until incipient deposition was achieved; that is, flow switches from non-deposition to incipient deposition. It was assumed that incipient deposition was satisfied when sediment particles were clustered visibly in certain areas at the channel bottom [15]. In this case, flow velocity is sufficiently low for incipient deposition of sediment. Incipient deposition was observed in the same form in trapezoidal and rectangular channels due to their flat bed. However, in the channels with U-shape and V-bottom, sediment particles were deposited in the center line of the channel with the same cross-fall. The form of the deposition depends on the channel bed. Sediment particles were accumulated on each other along the narrow centerline in the V-bottom channel, while accumulation in the circular and U-shape channels was not that narrow, as due to the wider bed along the centerline width, sediment particles spread over the bed width to make a deposited sediment layer instead.

## 4. Results

### 4.1. Shields Method

The incipient deposition experimental data of the channels are plotted on the Shields diagram (Figure 3), with the upper and lower limits as proposed by Paphitis [30]. Using the experimental data,  $\tau_{id}^*$  and  $Re^*$  were calculated using Equations (2) and (4), respectively, and functional relationships were developed by curve fitting to the measured data as

$$\tau_{id}^* = 0.74(Re^*)^{-0.86} \quad 3.13 < Re^* < 47.61 \quad r^2 = 0.913 \quad (9)$$

$$\tau_{id}^* = 0.32(Re^*)^{-0.97} \quad 2.36 < Re^* < 29.89 \quad r^2 = 0.953 \quad (10)$$

$$\tau_{id}^* = 0.57(Re^*)^{-0.83} \quad 3.02 < Re^* < 41.11 \quad r^2 = 0.972 \quad (11)$$

$$\tau_{id}^* = 0.55(Re^*)^{-0.72} \quad 3.19 < Re^* < 48.11 \quad r^2 = 0.960 \quad (12)$$

$$\tau_{id}^* = 0.79(Re^*)^{-0.78} \quad 3.46 < Re^* < 52.62 \quad r^2 = 0.907 \quad (13)$$

in the range  $2.36 < Re^* < 52.62$ . for the trapezoidal, rectangular, circular, U-shape, and V-bottom channels, respectively. In Equations (9)–(13),  $r^2$ , the determination coefficient, shows the goodness of fit of the curves. The data of the five channels are close to each other and partially overlap in some of the cases. It is seen from Figure 3 that, for the 0.15 mm- and 0.58 mm-particle size sands, incipient deposition shear stress remained above the upper limit of the Shields curve for the non-rectangular channels; however, in the rectangular channel, it is on the upper limit curve for the finest sand (the 0.15 mm-particle size sand) and on the average curve for the 0.58 mm-particle size sand. It should be kept in mind that the Shields curve has been developed for the incipient motion of sediment in loose boundary channels. Therefore, Figure 3 indicates, for sand finer than 0.58 mm, that the incipient deposition shear stress in rigid boundary channels is higher than the incipient motion shear stress in loose boundary channels. For sand with a 1.08 mm diameter, the incipient deposition shear stress remains between the upper limit and the average curve in the non-rectangular channels. It is on the lower limit curve in the rectangular channel case. It is also shown in Figure 3 that the incipient

deposition shear stress for the coarsest sand with a 1.52 mm diameter remains between the average and lower limit curves in all the channels other than the rectangular cross-section. It is below the lower limit curve for the rectangular channel. Generally, the incipient deposition shear stress of coarse sediment (1.08 mm and 1.52 mm) is lower than incipient motion shear stress in loose boundary channels. The coarser the sediment, the lower the shear stress under which the sediment particles initiate deposition within flow.

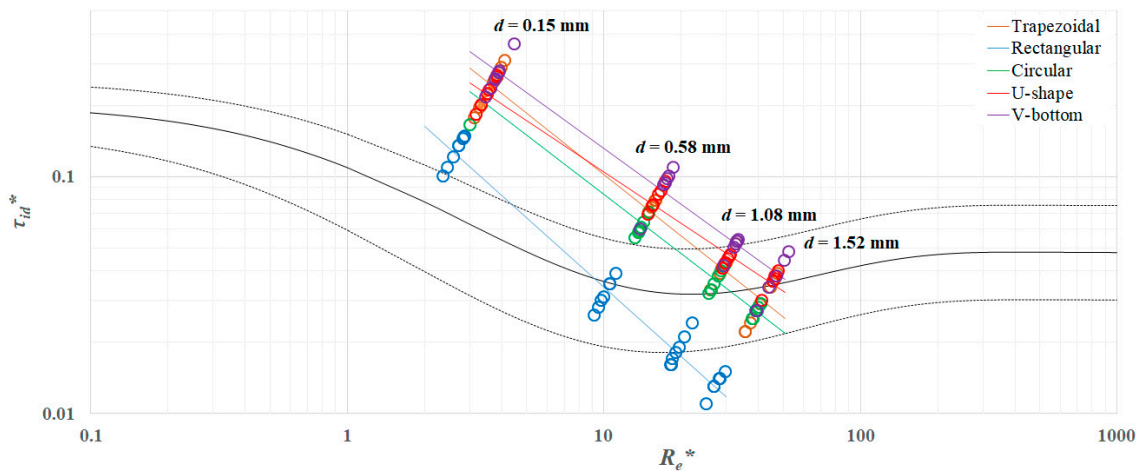


**Figure 3.** Relationship between the incipient deposition shear stress and Reynolds number based on the Shields method (circles show values calculated from the measurements, lines are the fitted equations).

It can also be seen that incipient deposition starts under lower shear stress in the rectangular channel (Figure 3). The incipient deposition shear stress of the trapezoidal, circular, U-shape, and V-bottom channels are close to each other. However, sediment particles in the V-bottom and U-shape channels initiate deposition under higher shear stress. The rectangular channel on the other hand obviously has different performance than the other channels; it allows sediment to move within flow until a lower shear stress is approached.

#### 4.2. Yalin Method

Incipient deposition experimental data are plotted on the Yalin diagram in Figure 4. For the five channels, the dimensionless incipient deposition shear stress ( $\tau_{id}^*$ ) and grain size ( $D_{gr}$ ) were calculated by Equations (2) and (8), respectively. Utilizing the incipient deposition experimental data,

$$\tau_{id}^* = 0.84D_{gr}^{-0.92} \quad r^2 = 0.913 \quad (14)$$

$$\tau_{id}^* = 0.47D_{gr}^{-0.99} \quad r^2 = 0.953 \quad (15)$$

$$\tau_{id}^* = 0.68D_{gr}^{-0.89} \quad r^2 = 0.972 \quad (16)$$

$$\tau_{id}^* = 0.65D_{gr}^{-0.80} \quad r^2 = 0.960 \quad (17)$$

$$\tau_{id}^* = 0.87D_{gr}^{-0.86} \quad r^2 = 0.907 \quad (18)$$

are proposed in the range of  $3.76 < D_{gr} < 38.06$  for the trapezoidal, rectangular, circular, U-shape, and V-bottom channels, respectively. It can be seen that the incipient deposition shear stress remains above the upper limit of the Yalin curve for the trapezoidal, U-shape, and V-bottom channels. It is on the upper limit for the fine sand ( $d = 0.15$  mm) in the rectangular channel. For the medium sand ( $d = 0.58$  mm) it is on and below the average curve in the circular and rectangular channels, respectively. For the coarser sand ( $d = 1.08$  mm), the incipient deposition shear stress remains between the upper limit and the average curve in the trapezoidal, U-shape, and V-bottom channels. It is below the lower

limit for the rectangular channel, and on the average curve for the circular channel. For the coarsest sand ( $d = 1.52$  mm), the incipient deposition shear stress is between the average curve and the lower limit in the channels with no rectangular cross-section. It is below the lower limit of the curve for the rectangular channel.

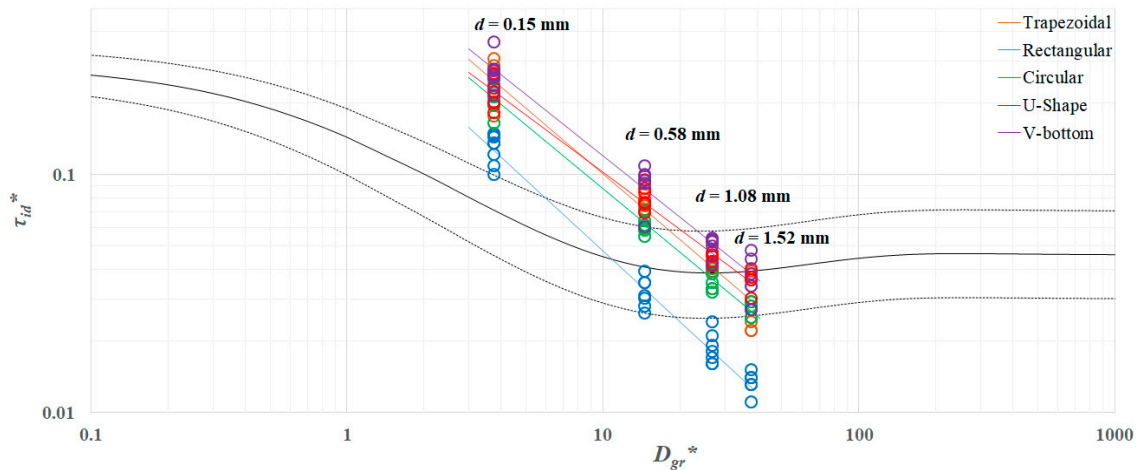


**Figure 4.** Relationship between the incipient deposition shear stress and grain size based on the Yalin method (circles show values calculated from the measurements, lines are the fitted equations).

The incipient deposition shear stress calculated from the experimental data (Figure 4) shows that sediment particles within flow in a rectangular channel start deposition under lower shear stress compared to the other channels. In other words, sediment particles within flow in the rectangular channel among the tested channels could be kept moving within flow under the lowest shear stress. The non-rectangular channels all have similar performance. Among the non-rectangular channels, the incipient deposition shear stress is lowest in the circular channel and the highest in the V-bottom channel. As a general result, it is clear that the coarser the sediment, the lower the shear stress under which sediment particles initiate deposition within flow. It can be said that the shape of the channel cross-section significantly affects the incipient deposition shear stress. Consequently, the incipient deposition shear stress is lower in the rectangular channel compared to the other channels.

## 5. Discussion

The results of the shear stress approach (Shields and Yalin methods) show that the channel cross-sectional shape significantly affects the incipient deposition shear stress. This is due to the change in the wall-normal component of the gravitational forces from which the friction force stems [31]. It is important to stress that the concept of incipient deposition is quite different to that of incipient motion. Not only the driving forces for the motion, but also the resisting forces against the motion are radically different in these two concepts. For the incipient motion, the friction coefficient is the static friction coefficient, which is accepted to be equal to the tangent of the friction angle between the bed and the grain (which becomes the angle of repose for a bed composed of identical particles). On the other hand, for incipient deposition, the friction coefficient is the dynamic friction coefficient, which is the tangent of the dynamic friction angle between the bed and the grain. Fredsoe and Deigaard [31] pointed out this important difference, and carried out an analysis for the correction of the transport rate of sediment particles moving on a transverse slope.

It should additionally be emphasized that, since the bed conditions in this study are smooth (i.e., the bed is the so-called “starving bed” where sediment particles travel on an otherwise hydraulically-smooth bed), one could expect that the changes with respect to the bed shape become even more pronounced compared to a regular bed composed of identical particles. Finally, it is possible to state that the critical shear stress curves for the incipient deposition for each of the given channel

cross-sections (trapezoidal, rectangular, circular, U-shape, and V-bottom) are expected to be different from each other, unless the channel is very wide, or unless a separate sophisticated correction for the critical shear stress for the deposition is carried out for each and every case. Such a correction, which was out of the scope of this study, should be expected to involve an averaging of the critical shear stress, possibly by integration across the channel cross-section.

The Shields and Yalin methods provide similar results. The behavior of the channels in terms of the magnitude of the incipient deposition shear stress does not change with the selected method. In both methods, the sediment particles initiate deposition under the lowest shear stress in the rectangular channel, and under the highest shear stress in the V-bottom channel. This is an expected result because the incipient deposition shear stress is calculated from the channel, sediment, and flow characteristics.

Another point worth discussing is the trend in the dimensionless incipient deposition shear stress against the particle Reynolds number in the Shields curve, and the grain size in the Yalin curve. The range of the experiments is  $2.36 < Re^* < 52.62$  for the Shields curve and  $3.76 < D_{gr} < 38.06$  for the Yalin curve. Within these ranges, both curves gradually decrease with increasing  $Re^*$  and  $D_{gr}$ . Experimental observation fits the general character of the Shields and Yalin curves within the range of the experiments.

It should also be mentioned that the incipient deposition shear stress decreases with increasing channel bed slope. In other words, sediment particles move within flow without being deposited until the shear stress becomes low enough to initiate deposition. Deposition starts under lower shear stress when the channel has a steeper slope. This is an observation for all sediment sizes and channel cross-sections.

One more point to discuss is the similarity with the velocity-based analysis of the incipient deposition performed by Aksoy et al. [26] under which the Novak-Nalluri [32] and Yang [33] methods were used. The rectangular cross-section channel was marked with the lowest velocity at the incipient deposition. Therefore, based on either the shear stress or the velocity approach, rectangular channels seem to be preferable.

Finally, as a general discussion, when the shear stress approach is compared with the velocity-based approach [26], there is a dilemma in the selection of the appropriate approach—shear stress or velocity. In the shear stress approach, two dimensionless parameters are used, namely the shear stress and the particle Reynolds number, both of which are dependent on shear stress; its critical value cannot be determined directly, but can only be calculated through a trial-and-error technique implicitly. In the velocity approach, critical velocity is calculated by an explicit solution. This gives an advantage to the velocity approach in terms of computation. However, as Vanoni [34] demonstrated, in using the velocity approach, flow depth or hydraulic radius, and in general channel cross-section, must be specified.

## 6. Conclusions

Incipient deposition is a different concept as opposed to the common assumption that the incipient deposition and incipient motion are the same. Therefore, the incipient deposition was considered solely in this study. An experimental analysis was performed for fixed bed channels with trapezoidal, rectangular, circular, U-shape, and V-bottom cross-sections. Experimental data was analyzed using the shear stress approach, under which the Shields and Yalin methods were considered to calculate the incipient deposition shear stress. Both methods showed that the incipient deposition starts under lower shear stress in the rectangular channel compared to the non-rectangular channels. This indicates that rectangular channels have higher efficiency of sediment transport as sediment particles deposit at lower velocities. This gives an advantage to rectangular channels in the design of urban drainage and sewer systems or irrigation canals. The trapezoidal, circular, U-shape, and V-bottom channels have similar performance, among which the circular channel has the lowest incipient deposition shear stress and the V-bottom channel has the highest. This makes the circular channel the second most preferable channel after the rectangular channel, and the V-bottom channel the least. Analysis brings

the conclusion that the cross-section of the channel significantly affects the shear stress at incipient deposition. The general trends in the Shields and Yalin curves were traced with the experimental data within the data range tested. One observation is that the incipient deposition shear stress decreases with the increasing channel bed slope; that is, sediment deposition in the channel is delayed when the channel has a steeper slope. The outputs of this study are expected to be considered together with the available literature and be employed for practical use in rigid boundary channel design. Further experiments are encouraged to extend the range of sediment size such that the validity range of the developed equations is increased.

**Funding:** The Scientific and Technological Research Council of Turkey (TUBITAK) Project number 114M283, The Scientific Research Projects (BAP) Unit of Istanbul Technical University Project number 37973.

**Acknowledgments:** The author is thankful to the Reviewers, Guest Editors and Academic Editor for their important comments with which the paper has been well improved.

**Conflicts of Interest:** The author declares no conflict of interest.

## References

1. Graf, W.H.; Acaroglu, E.R. Sediment transport in conveyance systems (Part 1)/A physical model for sediment transport in conveyance systems. *Hydrol. Sci. J.* **1968**, *13*, 20–39. [[CrossRef](#)]
2. Bogardi, J. *Sediment Transport in Alluvial Streams*; Akademiai Kiado: Budapest, Hungary, 1974.
3. Montanari, A.; Young, G.; Savenije, H.H.G.; Hughes, D.; Wagener, T.; Ren, L.L.; Koutsoyiannis, D.; Cudennec, C.; Toth, E.; Grimaldi, S.; et al. “Panta Rhei—Everything flows”: Change in hydrology and society—The IAHS scientific decade 2013–2022. *Hydrol. Sci. J.* **2013**, *58*, 1256–1275. [[CrossRef](#)]
4. Ceola, S.; Montanari, A.; Krueger, T.; Dyer, F.; Kreibich, H.; Westerberg, I.; Carr, G.; Cudennec, C.; Elshorbagy, A.; Savenije, H.; et al. Adaptation of water resources systems to changing society and environment: A statement by the International Association of Hydrological Sciences. *Hydrol. Sci. J.* **2016**, *61*, 2803–2817. [[CrossRef](#)]
5. McMillan, H.; Montanari, A.; Cudennec, C.; Savenije, H.; Kreibich, H.; Krüger, T.; Liu, J.; Meija, A.; van Loon, A.; Aksoy, H.; et al. Panta Rhei 2013–2015: Global perspectives on hydrology, society and change. *Hydrol. Sci. J.* **2016**, *61*, 1174–1191. [[CrossRef](#)]
6. Bong, C.H.J.; Lau, T.L.; Ghani, A.A.; Chan, N.W. Sediment deposit thickness and its effect on critical velocity for incipient motion. *Water Sci. Technol.* **2016**, *74*, 1876–1884. [[CrossRef](#)] [[PubMed](#)]
7. May, R.W.; Ackers, J.C.; Butler, D.; John, S. Development of design methodology for self-cleansing sewers. *Water Sci. Technol.* **1996**, *33*, 195–205. [[CrossRef](#)]
8. Butler, D.; May, R.; Ackers, J. Self-cleansing sewer design based on sediment transport principles. *J. Hydraul. Eng.* **2003**, *129*, 276–282. [[CrossRef](#)]
9. Safari, M.J.S.; Aksoy, H.; Unal, N.E.; Mohammadi, M. Non-deposition self-cleansing design criteria for drainage systems. *J. Hydro-Environ. Res.* **2017**, *14*, 76–84. [[CrossRef](#)]
10. Mayerle, R.; Nalluri, C.; Novak, P. Sediment transport in rigid bed conveyances. *J. Hydraul. Res.* **1991**, *29*, 475–495. [[CrossRef](#)]
11. May, R.W.P. *Sediment Transport in Pipes and Sewers with Deposited Beds*; Report SR 320; HR Wallingford: Wallingford, UK, 1993.
12. Ota, J.J.; Nalluri, C. Urban storm sewer design: Approach in consideration of sediments. *J. Hydraul. Eng.* **2003**, *129*, 291–297. [[CrossRef](#)]
13. Vongvisessomjai, N.; Tingsanchali, T.; Babel, M.S. Non-deposition design criteria for sewers with part-full flow. *Urban Water J.* **2010**, *7*, 61–77. [[CrossRef](#)]
14. Ota, J.J.; Perrusquia, G.S. Particle velocity and sediment transport at the limit of deposition in sewers. *Water Sci. Technol.* **2013**, *67*, 959–967. [[CrossRef](#)] [[PubMed](#)]
15. Loveless, J.H. Sediment Transport in Rigid Boundary Channels with Particular Reference to the Condition of Incipient Deposition. Ph.D. Thesis, University of London, London, UK, 1992.
16. Safari, M.J.S.; Aksoy, H.; Mohammadi, M. Incipient deposition of sediment in rigid boundary open channels. *Environ. Fluid Mech.* **2015**, *15*, 1053–1068. [[CrossRef](#)]

17. Safari, M.J.S.; Aksoy, H.; Mohammadi, M. Artificial neural network and regression models for flow velocity at sediment incipient deposition. *J. Hydrol.* **2016**, *541*, 1420–1429. [[CrossRef](#)]
18. Task Committee. Sediment transportation mechanics: Initiation of motion. *J. Hydraul. Div. ASCE* **1966**, *92(HY2)*, 291–314.
19. May, R.W.P. *Sediment Transport in Sewers*; Report No. IT 222; Hydraulic Research Station: Wallingford, UK, 1982.
20. Ackers, P. Sediment transport in sewers and the design implications. In Proceedings of the International Conference on Planning, Construction, Maintenance, and Operation of Sewerage Systems, Reading, UK, 12–14 September 1984; pp. 215–230.
21. Sanford, L.P.; Halka, J.P. Assessing the paradigm of mutually exclusive erosion and deposition of mud, with examples from upper Chesapeake Bay. *Mar. Geol.* **1993**, *114*, 37–57. [[CrossRef](#)]
22. Aksoy, H.; Safari, M.J.S. *Incipient Deposition of Sediment Particles in Rigid Boundary Channels*; Technical Report 113M062; Scientific and Technological Research Council of Turkey (TÜBİTAK): Istanbul, Turkey, 2014. (In Turkish)
23. Unal, N.E.; Aksoy, H.; Safari, M.J.S. *Self-Cleansing Drainage System Design by Incipient Motion and Incipient Deposition-Based Models*; Technical Report 114M283; Scientific and Technological Research Council of Turkey (TÜBİTAK): Istanbul, Turkey, 2016. (In Turkish)
24. Shields, A. *Application of Similarity Principles and Turbulence Research to Bed-Load Movement*; Translation from German; California Institute of Technology: Pasadena, CA, USA, 1936.
25. Yalin, M.S. *Mechanics of Sediment Transport*; Pergamon Press: Oxford, NY, USA, 1972.
26. Aksoy, H.; Safari, M.J.S.; Unal, N.E.; Mohammadi, M. Velocity-based analysis of incipient deposition in rigid boundary channels. *Water Sci. Technol.* **2017**, *76*, 2535–2543. [[CrossRef](#)] [[PubMed](#)]
27. Ippen, A.T.; Verma, R.P. *The Motion of Discrete Particles along the Bed of a Turbulent Stream: International Hydraulics Convention*; St. Anthony Falls Laboratory: Minneapolis, MN, USA, 1953; pp. 7–20.
28. Novak, P.; Nalluri, C. Sediment transport in smooth fixed bed channels. *J. Hydraul. Div. ASCE* **1975**, *101*, 1139–1154.
29. Butler, D.; May, R.W.P.; Ackers, J.C. Sediment transport in sewers Part 1: Background. *Proc. Inst. Civ. Eng.-Water Marit. Energy* **1996**, *118*, 103–112. [[CrossRef](#)]
30. Paphitis, D. Sediment movement under unidirectional flows: An assessment of empirical threshold curves. *Coas. Eng.* **2001**, *43*, 227–245. [[CrossRef](#)]
31. Fredsoe, J.; Deigaard, R. *Mechanics of Coastal Sediment Transport*; World Scientific: Singapore, 1992.
32. Novak, P.; Nalluri, C. Incipient motion of sediment particles over fixed beds. *J. Hydraul. Res.* **1984**, *22*, 181–197. [[CrossRef](#)]
33. Yang, C.T. Incipient motion and sediment transport. *J. Hydraul. Div. ASCE* **1973**, *99*, 1679–1704.
34. Vanoni, V.A. *Sedimentation Engineering*; American Society of Civil Engineers (ASCE): Reston, VA, USA, 2006.

